International Journal of Research in Engineering and Science (IJRES)
ISSN (Online): 2320-9364, ISSN (Print): 2320-9356
www.ijres.org Volume 11 Issue 2 ǁ February 2023 ǁ PP. 10-18

Experimental Analysis of Fluid Elastic Instability Impact of Flow Induced Vibration upon Wavy and Grooved Tubes within Heat Exchanger Tube Bundle

Muhammad Nouman Ali[a],Riffat Asim Pasha[b], Muhammad Ammar Akram[*,c,d], Muhammad Hammad Asghar[e], SyedaLaraibTariq[f,d], Majid Ali[g]

[a] *MS scholar, Mechanical Engineering Department, University of Engineering & Technology, Taxila, Punjab, Pakistan.*

[b] *Head of Department, Mechanical Engineering Department, University of Engineering & Technology, Taxila, Punjab, Pakistan.*

[c] *Corresponding Author. Lecturer, Mechanical Engineering Department, HITEC University Taxila, Punjab, Pakistan.*

[d] *PhD Scholar, Thermal Energy Engineering. U.S.-PAKISTAN Center For Advanced Studies In Energy (USPCASE), NUST Pakistan.*

[e] *Lab Engineer, Mechanical Engineering Department, HITEC University Taxila, Punjab, Pakistan.*

[f] *Lecturer, Mechanical Engineering Department, WAH Engineering College, University of WAH, Punjab, Pakistan.*

[g] *Head of Department, Thermal Energy Engineering. U.S.-PAKISTAN Centre For Advanced Studies In Energy (USPCASE), NUST Pakistan.*

Abstract:
The present study is concerned with the experimental analysis of fluid-elastic instability phenomenon of flow induced vibration of wavy and grooved tube in the heat exchanger tube bundle, considering the steady flow in the upstream of the tube array. Results are plotted and validated with the performed experimental results of tube bundle in parallel triangular arrangement with pitch to diameter ratio (1.54). The reduced gap velocity of tube bundle subjected to water tunnel ranges from 1.15 ≤ Ur ≤ 5.76 and Reynolds number ranges from 7.31 × 10^4 ≤ Re ≤ 1.83 × 10^5.

The monitored tube response in both stream wise and transverse direction seems to be highly dependent on its location in a specific row. First two rows of all tube's arrangement are found to be stable. Moreover, for wavy tube the third row is critical as it trigger's early instability in the monitored tube particularly in the transverse direction.

Keywords:
Vortex Shedding, Tube bundle, Wavy and Grooved Tubes, Parallel triangular, Fluid Elastic Instability, Flexible tube, Translational mode, Stiffness mechanism

---

Date of Submission: 23-01-2023 Date of acceptance: 06-02-2023

I. Introduction:

The interaction between the tubes of the heat exchanger causes vibration due to the flow. This interaction of the tube bundle with the upstream fluid can cause damage to the tube bundle. This failure can be the result of vortexshedding, acoustic resonance, frequency resonance and fluid-elastic instability. This type of phenomenon can lead to damage to the heat exchanger. The elastic instability of the fluid is our main concern as about 70% of failures in heat exchangers are due to this phenomenon.

The aim of the study was to investigate the effect of flow induced vibration of wavy andgrooved tubessurrounded by several discrete tubes in a water tunnel at different flowvelocities.Theexperimental results will be verified by published data. Our goal was to analyze the effects of fluid-elastic instability of heat exchanger tube bundles by varying tube geometry, tube shape and flow velocity.

II. Literature Review:

When there is a wavy plate, drag coefficient and lift coefficient vibration decrease by 27.5% and 54.9% respectively. The width of the wave stream is reduced and the length of the vortex formation is lengthened, indicating that the loss of the vortex has been prevented. Compared with a bare cylinder, two degrees of

freedom of flow-induced oscillations are estimated for a wide range of reduction velocities (Ur = 2–20). The corrugated sheet successfully suppresses the initial and lower branches of the vortex induced vibration, with a maximum reduction in the transverse flow amplitude of 92.44% (Zhu and Liu, 2020) [1].

Wavy axis cylinder with vortex shedding loss suppression provides excellent drag reduction. The drag decay disappears when Ma> 0.9, which is related to the coexistence of unstable and quasi-stable flow states and the generation of strongly oblique shock waves followed by a cylinder on the wavy axis. The turbulent oscillations in the posterior part near the cylinder with the wavy axis are very small for all Ma approaching infinity, resulting in a smaller oscillation force acting on the body(Xu *et al.*, 2020) [2].

At the same pump power, increasing the height of the waffle, imposing slots on the wavy fins can lead to an increase in heat resistance of 6-10°C. However, combining all three styles into a complex design can be much more effective. It is clearly more profitable to increase the length of the slots. The results show that the slots are 12mm long, 1mm wide, resulting in a 8-10% reduction in heat resistance(Sadeghianjahromi *et al.*, 2020) [3].

The $1.0 \leq \lambda/L_{mx} \leq 8.0$ range studied in this study includes both short and long wavelengths. The aspect ratio of the ellipse is between 0.5 and 1.0, making the body more streamlined as aspect ratio drops. At wavelengths in the unstable mode, the values of Strouhal number decrease rapidly. The formation of low Strouhal number is related to flow stability, as measured by shear elongation and suppression of decoupling of near-flow vortices(Nam and Yoon, 2021) [4].The vortex-split point in the slide line of the hyperbolic cylinder moves backward, resulting in a 27.6% reduction in drag. When the aspect ratio changed from 1 to 0.6, the drag of the stream parallel to the long axis decreased to 42.9%(Luo *et al.*, 2022)[5].

Compared with single cylinders, fixed wavy cylinders firmly reduce drag (average reduction of about 12.5%). Low mass damping systems find it difficult (if not impossible) to achieve the combination of VIV suppression and significant drag reduction. Smooth three-dimensional surfaces, which will create much less drag (like the current wavy cylinder), are not effective at fixing the meandering division lines needed to reduce excitement. Sharp surfaces can hold division lines in place in small lateral movements, but also increase drag proportionally(Assi and Bearman, 2018) [6].

Large-scale downstream vortices are generated near the flow due to the wavy geometry in the first two POD modes for $\lambda z/Dm = 1.89$ and 6.06. Meanwhile, the POD 3 mode shows that the wavy cylinder with the highest optimal $\lambda z/Dm = 6.06$ produces consistent dominant span and hairpin structures that break the saddle at frequencies different of people who separate themselves from the knot(Bai *et al.*, 2019) [7].

The presence of a giant cyclic bubble on the bottom of the saddle and the nodal planes confirms that the fluid forces have been significantly reduced. For the first time, different vortex separation frequencies are observed in the saddle and button, suggesting that the vortex structures separate from the saddle and knot at higher and lower frequencies, respectively. The vortexes in the direction of the time-averaged flow are concentrated between the saddle and the node in the plane of the cross-flow, forming an alternating pattern in the direction of the span(Bai, Zang and New, 2018) [8].

The wavy cylinder has better control over the vortex structure and a more stable development of the free shear layer, which can result in higher drag reduction and suppression of lift fluctuations. Wavy Cylinder without changing the cross-sectional shape or cylinder diameter, the vortex forces and vibrations caused by the flow can be greatly reduced, ensuring long-term and offshore drilling rig performance service life of risers and ducts. (Guo et al., 2019) [9]. Compared to the standard cylinder, drag and sound are reduced by 33.21% and 6,331 decibels, respectively(Karthik, Jeyakumar and Sebastin, 2021)[10].

The thermogas efficiency of round wavy pipes is better than that of straight round pipes due to the volumetric quality factor. Due to the total pressure drop in the tube, the value of Cp decreases as the fluid passes through the wavy circular tube. Due to the increasing influence of convection, the local Nusselt number increases as the Reynolds number increases. The overall distribution of the local Nusselt number decreases as we pass through the wavy tube, due to the growth of the thermal boundary layer in the direction of the stream(Kim *et al.*, 2015) [11].

The drag coefficient of wavy cylinders is lower than that of round cylinders, which reduces drag by up to 20%. The oscillating root mean square lift coefficient of the wavy cylinder was also found to be significantly lower than that of the rounded cylinder. The Strouhal number of the wavy cylinder is roughly the same as that of the corresponding circular cylinder, according to the spectral analysis of the hot wire and the load cell signal(Lam *et al.*, 2004) [12].

A row of five circular cylinders, staggered wavy cylinders and unstaggered corrugated cylinders adjusted to pitch to diameter ratio(P/D = 1.5) with Re varying from 125 to 40,000. . vortex closing length, depending on the result(Lam *et al.*, 2007) [13].

Numerical and experimental studies of round and wavy cylinders are carried out. Both laminar and turbulent flows have been studied. In general, the use of such preparations does not reduce drag in turbulent flows.This kind of fluid structure interaction reduces the impact behind the front row tubes. As a result, the impact force on the second row of seats will be reduced. Vibrations caused by cross-flow of a large number of

tube bundles in heat exchangers can be controlled using corrugated tube designs(Lam *et al.*, 2008) [14].

It was observed that for Reynolds numbers ranging from 6800 to 13400, there was a decrease in drag and cancel the variable lift of a wavy cylinder, comparable to what happens in laminar flow. The corrugated cylinder in the tube bundle can help to reduce the vibration caused by the flow of the tube bundle in the heat exchanger(Lam *et al.*, 2009) [15].

III. Modeling and Design

Root mean square amplitude can be found as;

$$A_{rms} = 0.707 \frac{A_{p-p}}{2}$$

Resultant amplitude can be calculated as;

$$A = \sqrt{{A_{sw}}^2 + {A_{tr}}^2}$$

Where

A_{sw} = Stream wise direction amplitude

A_{tr} = Transverse direction amplitude

A= Resultant amplitude

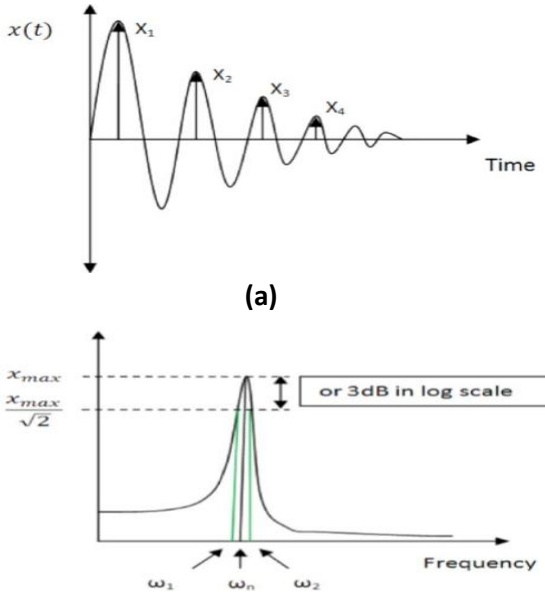

Fig 1 (a) Logarithmic decrement method (b) Bandwidth method

Damping factor can be calculated using logarithmic method as;

$$\delta = \frac{1}{n} ln \left(\frac{x_1}{x_{n+1}}\right)$$

$$\zeta = \frac{\delta}{\sqrt{4\pi^2 + \delta^2}}$$

Where

x_1 = First cycle amplitude

x_{n+1}= nth cycle amplitude

Damping ratio can be found as;

$\zeta = \frac{\omega_2 - \omega_1}{2\omega_n}$

The log reduction (δ) for lightly damped structures such as shell and tube damping can be calculated as follows:

$$\delta \cong 2\pi\zeta$$

Mass damping parameter $MDP = \frac{m(2\pi\zeta)}{\rho D^2}$

Formula for Reynolds Number Calculation:
Reynolds number = (Fluid velocity x Hydraulic diameter) / Kinematic viscosity
V_1= 0.32m/s, V_2= 0.80m/s, D_h= 0.2286, ν= 10^{-6} m^2 /s, Re_1= $V_1 \times D_h/v$,Re_1=0.073152×10^6
Re_2= $V_2 \times D_h/v$, Re_2=0.18288 ×10^6
Wavy Tube

D_{max}= 12mm

D_m = 10mm

D_m = (D_{max} +D_{min})/2

=12+D_{min}/2 =10mm
D_{min}= 20-12= 8mm

Assume λ= 40mm , a=1.5mm

a/D_m = 0.15mm

λ/D_m = 40/10 = 4mm

P/D_{max}=1.54
P= 1.54*12 = 18.48

Fig 2 Design of Wavy Tube on Solid works

Groove Tube:
Depth of Groove = 2 mm
Width of Groove = 1mm

Fig 3 Grooved Tube Diameter with grooved slots `.

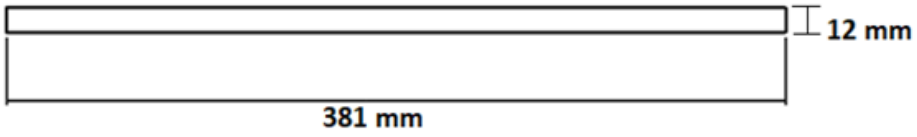

Fig 4 Grooved Tube Length

Fig 5Experimental Groove & Wavy Tube

IV. Experimental Setup

The experiment was conducted in a water tunnel, as shown in Figure. The water tunnel takes water from the reservoir and flows it through the tunnel test section. After the water passes through the measuring part, itflow out to the Reservoir. A Gate valve is placed to vary the velocities of the fluid. The figure below shows the water tunnel used for the experiment.

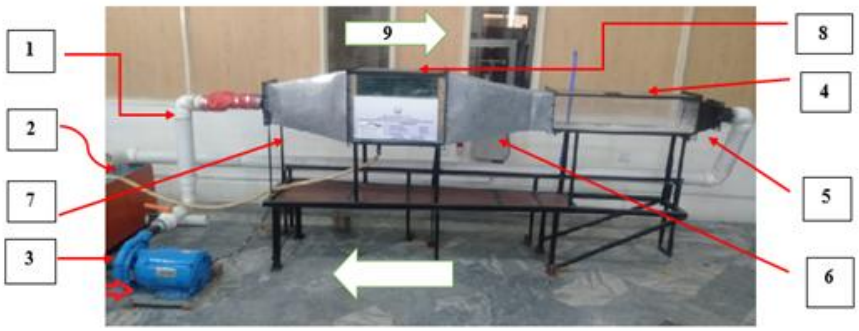

Fig 6 Water Tunnel

Table 1 Water Tunnel Labeling

1.Plumbing system	2. Water Reservoir	3. Water Pump
4. Test Section	5.Bend with Turning vanes	6.Contraction
7. Diffuser	8. Baffles	9.Flow Direction

Table 2 Experimental Tube Bundle Specifications

Pitch to Diameter Ratio (P/D)	**1.54**
Tube bundle arrangement of Tube Bundle	Parallel triangular
Tube outer diameter (d_o)	12 mm
Rows	4
Mass of the monitored tube including the mass of accelerometer (m_t)	181 ± 1 g
Length of the monitored tube (L_t)	381 mm
Mass of surrounding flexible tubes (m_{st})	181 ± 1 g
Length of surrounding flexible tubes (L_{st})	284.5 mm
Tube Material	Aluminum
Fluid type	water

This experiment was performed with a pitch ratio of 1.54 (parallel triangular tube arrangement) for Grooved and Wavy tube. For single flexible tube bundles, an accelerometer was attached to the top of the flexible tube with the help of piano wire and frequency was tuned between 8-9 Hz by controlling piano wire stiffness. Triaxial Micro-strain accelerometer was attached at the top of flexible tube to monitor tube vibration.

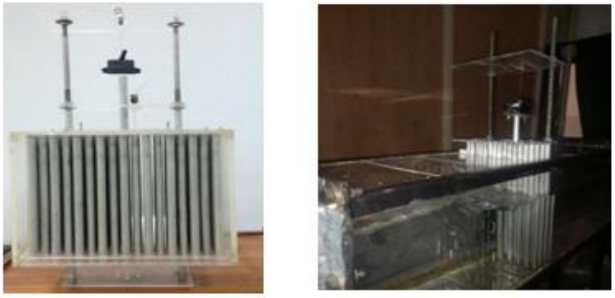

Fig 7 Tube Bundle

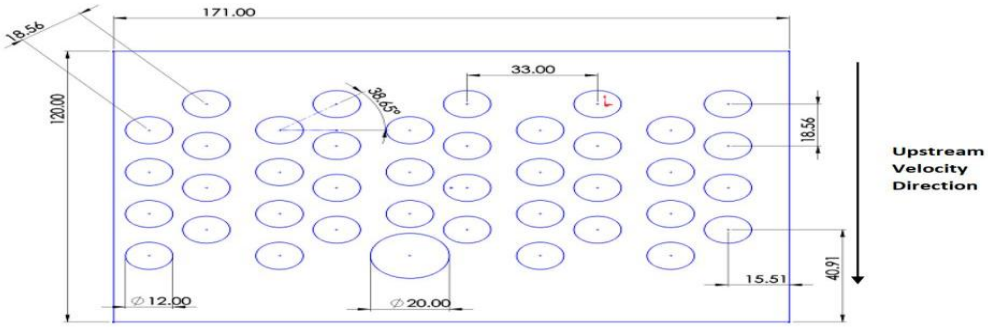

Fig 8 Tube bundle drawing with parallel triangular arrangement with P/D of 1.54

Fig 9 Tube bundle CAD Model with parallel triangular arrangement with P/D of 1.54

Axis and Channel No's:

X-axis: Channel 2 (Red)

Y-axis: Channel 1 (Green)

Z-axis: Channel 3 (Blue)

- **Channel 2 shows the drag force values**
- **Channel 1 shows the lift force values**

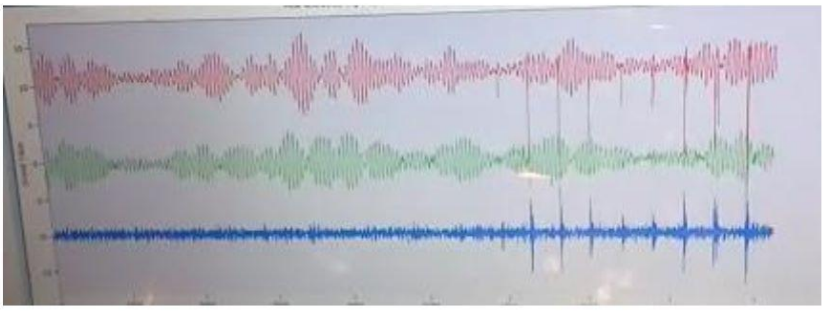

Fig 10 Node Commander Signal

V. Results and Discussions

The results in the form of amplitude response and frequency spectrum show the behavior of the tube in the array.This presents step-by-step data analysis of an experiment performed with a pitch t ratio of 1.54 (parallel triangular tube arrangement) for a tube bundle. Instability of single flexible tube in a rigid network is highly dependent on the position of the tube.

Amplitude Response of Wavy Tube:

The instability observed in both the stream and transverse directions for the tube was monitored when placed in the first row of the tube bundle at a pitch ratio of 1.54 and the peak amplitude was still lower at 1.44% in the stream wise direction of the diameter of the tube (a). For the first row, however, the monitored tube experiences instability at a reduce velocity of 3.5 in the direction of the fluid stream. For the second row (b), the margin is less than 1.26% of the pipe diameter achieved by the tracked tubeboth in the transverse direction at a Reduction Rate of 4.61%. The same is true for the third row (c) in part because the monitored tube experiences instability in the transverse direction with the same reduced velocity of about 5.76 with a peak amplitude reaching 1.46% of the tube dia. In the fourth row (d), tube vibration is reduced and intensity is 1.02% with a reduction rate of 4.61 %.

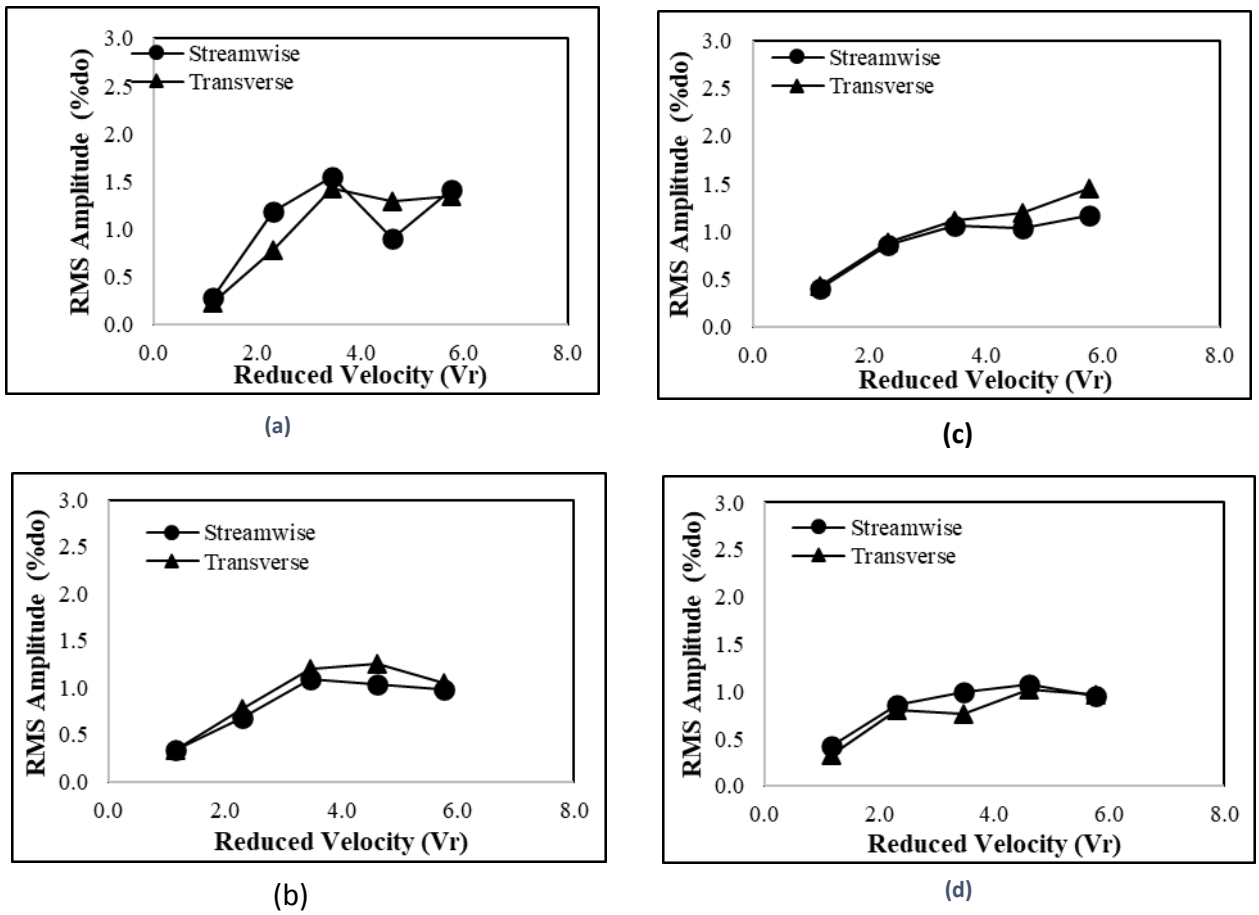

Fig 8 Amplitude response of Wavy tube in parallel triangular tube bundle with pitch ratio of 1.54 at when the tube is placed in (a) First row (b) Second row (c) Third row (d) Fourth row.

Amplitude Response of Grooved Tube:

The instability observed in both the stream wise direction and the transverse direction for the tube was monitored when placed in the first row of the tube bundle and the peak amplitude remained below 1.05% of the tube diameter (yes). However, for the first row, the monitored tube experienced instability at a reduced velocity near 3.45 in the transverse direction and in the direction of the stream wise.

For the second row (b), the 1.19% amplitude of the pipe diameter achieved by the tube is tracked in the direction of the stream wise and shows instability at a reduced rate of 4.61%. This is also true for the third row (c) partly because the monitored tube experiences instability in both the stream wise and transverse directions at

the same rate of decrease of about 5.76% with peak amplitude reaching up to 1.55% in the direction of stream in the direction of the pipe diameter with a reduced velocity of 5.67.

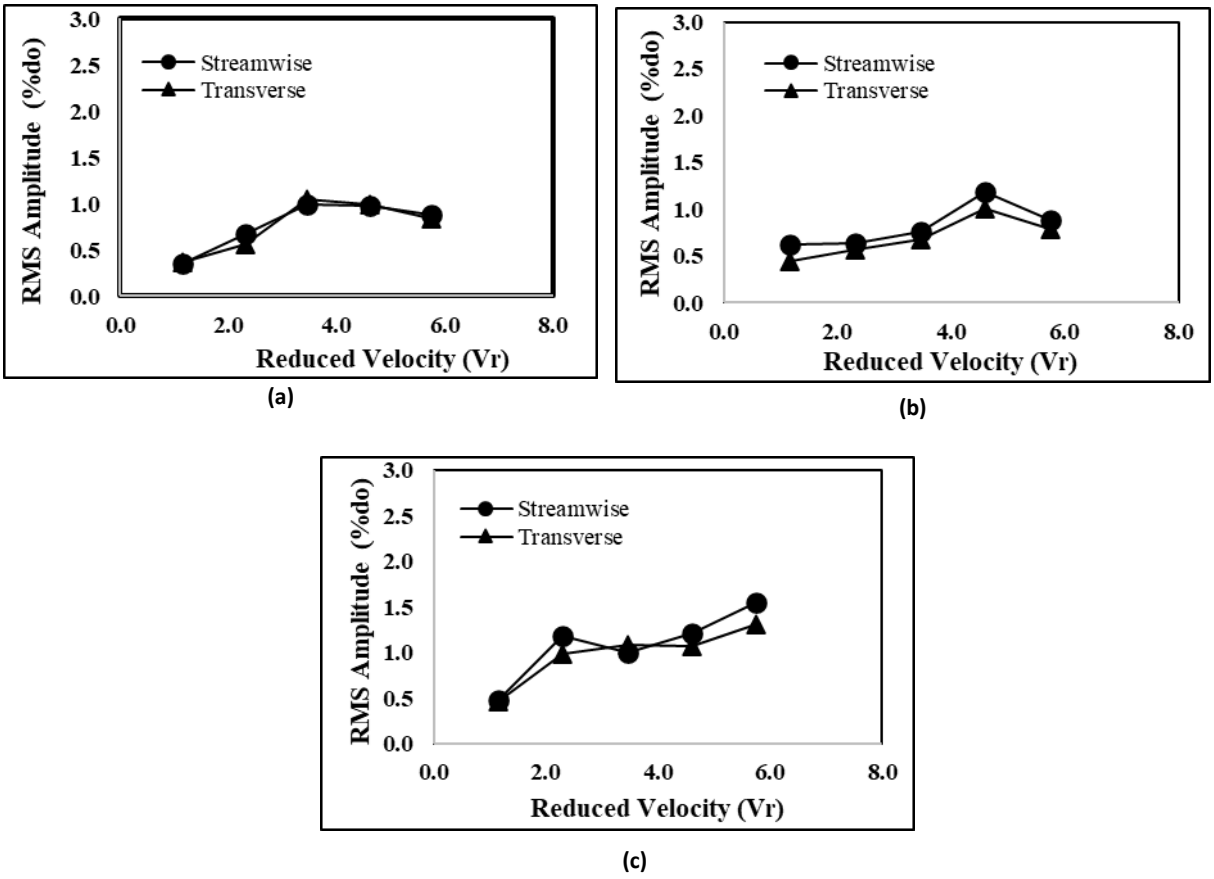

Fig 9 Amplitude response of Groove tube in parallel triangular tube bundle with pitch ratio of 1.54 at when the tube is placed in (a) First row (b) Second row (c) Third row.

VI. Conclusion

This study is concerned with the experimental analysis of fluid-elastic instability phenomenon impact of FIV upon wavy and grooved tube within a heat exchanger tube bundlesubjected to steady flow with various flow velocities and its validation with performed experimental analysis of the parallel triangular tube bundle with 1.54 pitch ratios, in water tunnel.The effect of flow velocities and tube location on the instability threshold is assessed.

- The monitored tube response in both stream wise and transverse direction seems to be highly dependent on its location in a specific row. The first two rows of all tube's arrangement are found to be stable. Moreover, for wavy tube the third row is less critical as compared to plane tube because it triggersless instability in the monitored tube particularly in the transverse direction.
- Stabilization effect was observed with maximum tube amplitude remains less than 1.46% of tube diameter for a single flexible tube in a rigid tube bundle of parallel triangular tube arrangement with ratio of 1.54, and instability was delayed with an increase in flow intensity.
- Grooved tube was found to be more stable in all rows of tube bundle. The amplitude of the first two rows of tube's arrangement is found to be stable. Moreover, For Grooved tube the third row is more excited as compared to first two rows, but stability was observed in the Grooved tube particularly in the stream wise direction. This study can help to improve the design guidelines for heat exchangers. It can reduce pressure drops and hence heat transfer rate enhancement can be obtained with more reliability in the designed product.

REFERENCES

[1]. Zhu, H. and Liu, W. (2020) 'Flow control and vibration response of a circular cylinder attached with a wavy plate', Ocean Engineering, 212(April), p. 107537. doi: 10.1016/j.oceaneng.2020.107537.

[2]. Xu, C. Y. et al. (2020) 'Effect of Mach number on the compressible flow past a wavy-axis cylinder', Aerospace Science and

Technology, 104(M). doi: 10.1016/j.ast.2020.105943.
[3]. Sadeghianjahromi, A. et al. (2020) 'Heat transfer enhancement of wavy fin-and-tube heat exchangers via innovative compound designs', International Journal of Thermal Sciences, 149(June 2018), p. 106211. doi: 10.1016/j.ijthermalsci.2019.106211.
[4]. Nam, S. H. and Yoon, H. S. (2021) 'Effect of the wavy geometric disturbance on the flow over elliptic cylinders with different aspect ratios', Ocean Engineering, 243(September 2021), p. 110287. doi: 10.1016/j.oceaneng.2021.110287.
[5]. Luo, J. L. et al. (2022) 'Numerical study of the flow around a hyperbolic cylinder at Reynolds number 3900', Ocean Engineering, 246(September 2021), p. 110669. doi: 10.1016/j.oceaneng.2022.110669.
[6]. Assi, G. R. S. and Bearman, P. W. (2018) 'Vortex-induced vibration of a wavy elliptic cylinder', Journal of Fluids and Structures, 80, pp. 1–21. doi: 10.1016/j.jfluidstructs.2018.02.007.
[7]. Bai, H. L. et al. (2019) 'The near wake of sinusoidal wavy cylinders: Three-dimensional POD analyses', International Journal of Heat and Fluid Flow, 75(June 2018), pp. 256–277. doi: 10.1016/j.ijheatfluidflow.2019.01.013.
[8]. Bai, H. L., Zang, B. and New, T. H. (2018) 'The near wake of a sinusoidal wavy cylinder with a large spanwise wavelength using time-resolved particle image velocimetry', Experiments in Fluids, 60(1), pp. 1–18. doi: 10.1007/s00348-018-2664-3.
[9]. Guo, C. et al. (2019) 'Large eddy simulation of flow over wavy cylinders with different twisted angles at a subcritical reynolds number', Journal of Marine Science and Engineering, 7(7). doi: 10.3390/jmse7070227.
[10]. Karthik, K., Jeyakumar, S. and Sebastin, J. S. (2021) 'Optimization of wavy cylinder for aerodynamic drag and aeroacoustic sound reduction using computational fluid dynamics analysis', Proceedings of the Institution of Mechanical Engineers, Part C: Journal of Mechanical Engineering Science, 235(11), pp. 1979–1991. doi: 10.1177/0954406220950353.
[11]. Kim, Y. J. et al. (2015) 'Numerical study of fluid flow and convective heat transfer characteristics in a sinusoidal wavy circular tube', Journal of Mechanical Science and Technology, 30(3), pp. 1185–1196. doi: 10.1007/s12206-016-0222-6.
[12]. Lam, K. et al. (2004) 'Experimental investigation of the mean and fluctuating forces of wavy (varicose) cylinders in a cross-flow', Journal of Fluids and Structures, 19(3), pp. 321–334. doi: 10.1016/j.jfluidstructs.2003.12.010.
[13]. Lam, K. et al. (2007) 'Flow characteristics around a row of circular and wavy cylinders', Journal of Mechanical Science and Technology, 21(11), pp. 1910–1917. doi: 10.1007/BF03177448.
[14]. Lam, K. et al. (2008) 'Investigation of Flow Characteristic'S in Heat Exchanger Tube Bundles Composed of Wavy and Circular Cylinders', Flow-Induced Vibration, 15, p. 217+.
[15]. Lam, K. et al. (2009) 'Experimental study and large eddy simulation of turbulent flow around tube bundles composed of wavy and circular cylinders', International Journal of Heat and Fluid Flow, 31(1), pp. 32–44. doi: 10.1016/j.ijheatfluidflow.2009.10.006.